

The first layered analogue of Sr₂FeMoO₆; the structure and electronic properties of Sr₄FeMoO₈

Edmund J. Cussen^{*a} and Mike F. Thomas^b

Received 26th October 2004, Accepted 21st December 2004

First published as an Advance Article on the web 17th January 2005

DOI: 10.1039/b416470a

The $n = 1$ Ruddlesden–Popper phase Sr₄FeMoO₈ has been synthesised by high temperature ceramic methods under reducing conditions. Rietveld refinements of the structure against X-ray and neutron powder diffraction data shows that this phase adopts the space group *I4/mmm* ($a = 3.92962(5)$, $c = 12.6707(2)$ Å) and contains a crystallographically disordered arrangement of Fe and Mo on the single octahedral site in the structure. Mössbauer spectroscopy data show that iron is in the trivalent state and that the transition metals are fully disordered at a local scale. SQUID magnetometry measurements and low temperature neutron diffraction experiments have been used to examine the magnetic properties of this material. The magnetic susceptibility shows Curie–Weiss paramagnetism above a magnetic transition at 16(1) K. Below this temperature the sample shows magnetic hysteresis, but the neutron diffraction data show no evidence of the additional Bragg intensity associated with the formation of a magnetically ordered phase. The magnetic transition at 16 K is therefore assigned to the formation of a spin-glass phase. The absence of magnetic order in this material is due to the chemical disorder in the Fe/Mo occupancy of the octahedral site and thus the randomisation of the magnetic exchange interactions.

Introduction

Double perovskites, A₂BB'O₆ (where A is a divalent cation and B and B' are typically transition metals) have been studied since the 1960s¹ due to the wide-ranging electronic properties which can be developed as a function of variation in composition, oxidation state, chemical cation order and structural distortion. Recently, a resurgence in interest in these materials has been driven by the report of room temperature magnetoresistance in Sr₂FeMoO₆.² The oxidation states of the transition metals in this compound have been the subject of considerable debate and it is now recognised that these are most accurately described using a non-integer description Fe^{(3-x)/Mo^(5+x)}, *i.e.* some unpaired electron density is associated with the molybdenum cations. Sr₂FeMoO₆ contains cation-ordered Fe and Mo giving rise to ferrimagnetic ordering below $T_c = 420$ K. Below this temperature the Fe electrons remain localised in a parallel arrangement whilst the fully polarised electrons associated with Mo are delocalised leading to semi-metallic behaviour. This gives rise to the inter-grain tunnelling,³ magnetoresistive effect. Since this observation was reported, a large number of publications have arisen⁴ which feature cation substitution for Sr, Fe and Mo.^{5–8} Despite these efforts, no substantial enhancement of the magnetoresistive effect has been observed and the effect has only been reproduced in Sr₂FeReO₆.⁹ This is due to the difficulty of synthesising compounds which contain the crucial components which give rise to the magnetoresistive effect in Sr₂FeMoO₆; the presence of chemical cation ordering between two cations which each contain non-zero d-orbital occupancies. The latter condition is proving problematic: the substitution of other 3d

metals for Fe³⁺ can give rise to the formation of an M²⁺/Mo⁶⁺ ion pair.^{10–12} This introduction of a 4d⁰ metal centre into the magnetic exchange pathway prevents the formation of a ferrimagnetic structure and instead gives rise to antiferromagnetic order at reduced temperature. Substitution of tungsten for molybdenum has a similar effect¹³ (due to the more reducing nature of W⁵⁺ compared to Mo⁵⁺) and Sr₂FeWO₆ contains Fe²⁺/W⁶⁺ which again precludes ferrimagnetic ordering. Despite the intensive interest in this area there has been little research into non-perovskite phases which contain similar arrangements of cations. A heavily distorted zirconolite phase has recently been reported¹⁴ but, due to a disordered arrangement of Fe and Mo, failed to reproduce the properties of the perovskite.

We have chosen to examine analogues of the perovskite in the Ruddlesden–Popper (RP) family of materials, where cation-order between octahedrally coordinated metals has been observed in a number of systems.^{15–17} The RP structures contain a variable number (n) of layers of perovskite structure separated by a layer of rock salt, as shown for $n = 1$ in Fig. 1, which can give rise to highly anisotropic electronic properties.¹⁸ It is anticipated that the rock salt layers of the RP phases may disrupt the magnetic order between the perovskite blocks. As the magnetoresistive effect in Sr₂FeMoO₆ depends on the concentration of magnetic domain boundaries,³ this limiting of the magnetic order in one dimension could give rise to a considerable enhancement of the magnetoresistive effect compared to that observed in the three-dimensional perovskite. In this article we report the structural and electronic properties of the $n = 1$ phase Sr₄FeMoO₈. In addition to being the first layered perovskite analogue of Sr₂FeMoO₆, this represents the first structural characterisation of a RP molybdate and is the first

^{*}edmund.cussen@nottingham.ac.uk

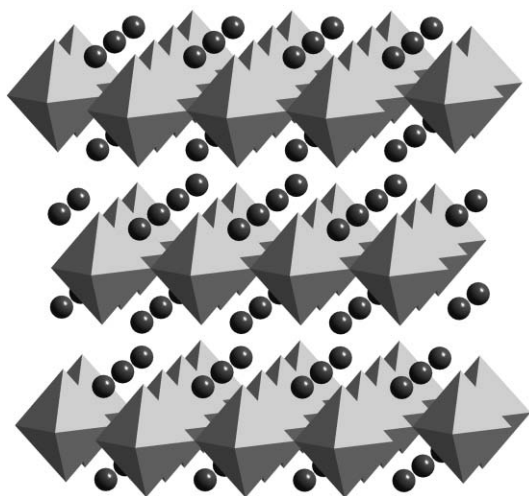


Fig. 1 The $n = 1$ Ruddlesden–Popper structure of $\text{Sr}_4\text{FeMoO}_8$. Grey spheres and octahedra represent Sr cations and Fe/MoO_6 units respectively.

in a potential family of cation-doped materials based on Sr_2MoO_4 .

Experimental

The initial synthesis of $\text{Sr}_4\text{FeMoO}_8$ proceeded using a typical solid state preparation. Stoichiometric quantities of SrCO_3 , MoO_3 and Fe_2O_3 were intimately ground, pressed into a pellet and heated in air at $1\text{ }^\circ\text{C min}^{-1}$ from $600\text{ }^\circ\text{C}$ to $800\text{ }^\circ\text{C}$ and held at this temperature overnight. The pellet was then re-ground and heated at $1050\text{ }^\circ\text{C}$ under a flowing atmosphere of 5% $\text{H}_2/95\%$ N_2 for a total of 5 days. During this time the sample was cooled to room temperature, ground and re-pelleted several times to give sample **A**. The sample prepared in this manner was found to contain small quantities of impurity phases. Subsequent to this discovery, the preparation was repeated using 10 wt.% excess of MoO_3 and the pellet was heated from $500\text{ }^\circ\text{C}$ to $900\text{ }^\circ\text{C}$ in air at $0.5\text{ }^\circ\text{C min}^{-1}$. During this heating the pellet was surrounded by powder of the same stoichiometry. The pellet was then ground and heated from $900\text{ }^\circ\text{C}$ to $1200\text{ }^\circ\text{C}$ at $2\text{ }^\circ\text{C min}^{-1}$ under 2.5% $\text{H}_2/97.5\%$ N_2 and then held at $1200\text{ }^\circ\text{C}$ for 2 days to give sample **B**.

The progress of these reactions were followed by X-ray powder diffraction using a Philips Xpert diffractometer operating with $\text{Cu K}\alpha$ radiation. Data were collected in the range $10 \leq 2\theta/^\circ \leq 90$. Neutron powder diffraction data were collected from *ca.* 5 g of sample **A** contained in a cylindrical vanadium can using the time-of-flight diffractometer Polaris at the ISIS facility, Rutherford Appleton Laboratories. Data were collected in the range $0.4 \leq d/\text{\AA} \leq 8.0$. The sample temperature was controlled using an ILL orange cryostat and the data were analysed using the Rietveld method¹⁹ as implemented in the GSAS suite²⁰ of programs. The background was described by a shifted Chebyshev function and the peak shape was modelled using a convolution of exponential and pseudo-Voigt functions.

Magnetic susceptibility data were collected using a Quantum Design MPMS SQUID magnetometer from samples contained

within gelatine capsules after cooling the sample in either zero applied field or the measuring field of 1000 G. Mössbauer spectroscopy data were collected using a transmission spectrometer and the values of the isomer shift are reported with respect to α -iron at 300 K.

Results

X-Ray powder diffraction data collected from sample **A** revealed a quantity of SrO impurity (1.1(1) wt.%) which could not be eliminated with further heating. The remaining peaks in the pattern could be indexed using a structural model based on that reported for Sr_2FeO_4 in the space group $I4/mmm$. This structure contains only a single transition metal site and so indicates the absence of crystallographic cation order between molybdenum and iron. Bulk magnetometry measurements were dominated by a small quantity of material showing a large, temperature independent magnetisation which prevented any assignment of the magnetic properties to the target phase $\text{Sr}_4\text{FeMoO}_8$.

The scattered intensity of X-rays varies as a function of the square of the number of electrons and for $\text{Sr}_4\text{FeMoO}_8$ this makes X-ray diffraction a relatively insensitive technique for the determination of the positions, occupancy and displacement parameters of the oxide ions. Therefore, this sample was examined using neutron powder diffraction. The data collected at room temperature indicated that the sample contained a small quantity of metallic iron impurity and some small additional broad reflections arising from $\text{Sr}(\text{OH})_2 \cdot \text{H}_2\text{O}$. Including Fe 2.7(3) wt.%, SrO 3.5(5) wt.% and 3.5(2) wt.% $\text{Sr}(\text{OH})_2 \cdot \text{H}_2\text{O}$ in the Rietveld refinement allowed a reasonable fit to be achieved to the data using the crystallographic model determined from the X-ray data as a starting point for the refinement. Despite the presence of impurity phases, the quality of the data was such that it was possible to refine anisotropic displacement parameters where the site symmetry permitted and the refinement readily refined to convergence. The oxide ion fractional occupancies were allowed to vary freely and refined to values which did not depart significantly from unity. Therefore they were subsequently fixed at this value. The converged refinement shown in Fig. 2 yielded the fit

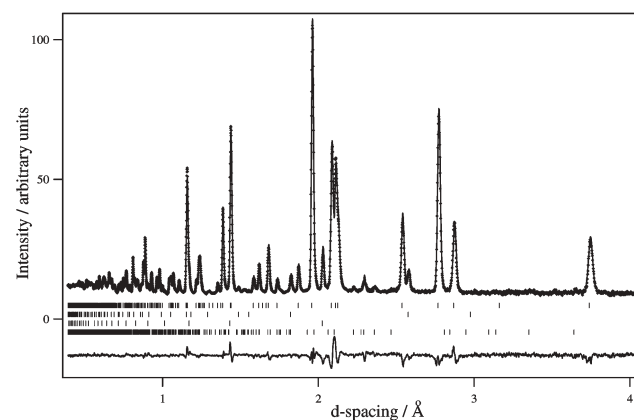


Fig. 2 Observed (dots), calculated (line) and difference neutron powder diffraction patterns from $\text{Sr}_4\text{FeMoO}_8$ collected from sample **A** at room temperature.

parameters $R_{wp} = 3.02\%$, $R_p = 4.40\%$, and $\chi^2 = 7.18$ using a total of 57 variables; 4 lattice parameters, 3 phase fractions, 3 histogram scale factors, 4 zero point parameters, 2 positional parameters, 8 displacement parameters, 14 profile parameters and 19 background parameters. The atomic parameters and bond lengths resulting from this fit are summarised in Tables 1 and 2. Neutron powder diffraction data were also collected as a function of temperature in the range $1.7 \leq T/K \leq 34.6$ in order to establish the existence or otherwise of a magnetically-ordered low temperature phase. The data collected at 1.7 K showed no substantial difference from the data collected at room temperature and could be satisfactorily fitted using the same structural model indicating that the Bragg peaks are purely nuclear in origin. The resulting atomic distances are summarised in Table 2. Further neutron diffraction patterns were collected as function of temperature. These data sets were fitted using the same structural model indicating no substantial changes occurred in the structure as a function of temperature. Close examination of structural parameters resulting from these refinements showed a smooth evolution with temperature for displacement parameters and lattice parameters. The bond lengths showed no significant change in the temperature range $1.7 \leq T/K \leq 34.6$ except for the distance between the transition metal site and the apical oxide ion. As shown in Fig. 3, this distance undergoes a small, but statistically significant reduction in the bond length as a function of temperature on heating from 17.0(1) to 19.8(1) K. This bond length has a mean value of 2.0265(3) Å for temperatures ≤ 17 K but 2.0251(2) Å in the range $19.8 \leq T/K \leq 34.6$.

The Mössbauer spectroscopy data collected from sample A are shown in Fig. 4. At room temperature the data can be fitted using a pair of doublets with isomer shifts of 0.31(1) and 0.49(1) mm s^{-1} . Close examination of these data in the regions of +6 mm s^{-1} and -6 mm s^{-1} where the contribution from metallic iron would be strongest²¹ showed that the metallic iron impurity identified in the neutron diffraction data was undetectable in the Mössbauer spectroscopy experiment. On cooling the sample to 77 K, both of these doublets move to

Table 1 Atomic parameters derived for $\text{Sr}_4\text{FeMoO}_8$ from neutron powder diffraction data collected at room temperature

Atom	Site	<i>x</i>	<i>y</i>	<i>z</i>	$100U_{11}$	$100U_{22}$	$100U_{33}^a$
Sr	4e	0	0	0.35330(4)	0.914(13)	0.914(13)	0.39(2)
Fe/Mo	2a	0	0	0	0.335(8) ^b		
O(1)	4c	0	1/2	0	0.82(3)	0.24(2)	1.06(3)
O(2)	4e	0	0	0.15971(5)	1.16(2)	1.16(2)	0.53(3)

^a U_{12} , U_{13} and U_{23} are constrained to zero by site symmetries.

^b Isotropic temperature factor.

Table 2 Bond lengths derived for $\text{Sr}_4\text{FeMoO}_8$ from neutron powder diffraction data collected at room temperature and 1.7 K

Bond	Distance (RT)/Å	Distance (1.7 K)/Å
Sr–O(1)	$2.7015(4) \times 4$	$2.6943(4) \times 4$
Sr–O(2)	2.4528(8)	2.4439(8)
Sr–O(2)	$2.77720(6) \times 4$	$2.76959(7) \times 4$
Fe/Mo–O(1)	$1.96031(2) \times 4$	$1.95461(3) \times 4$
Fe/Mo–O(2)	$2.0237(6) \times 2$	$2.0265(7) \times 2$
mean Fe/Mo–O	1.98144	1.97857

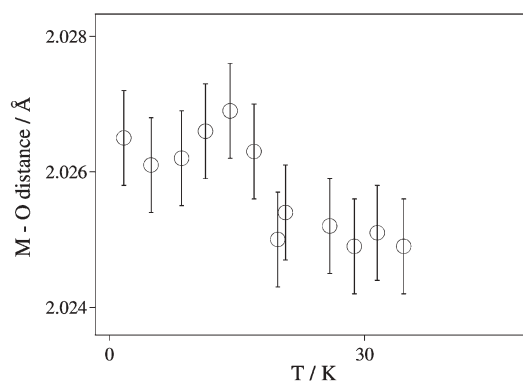


Fig. 3 The variation in distance from the transition metal site to the apical oxide ion position as a function of temperature in $\text{Sr}_4\text{FeMoO}_8$ derived from the Rietveld refinement with the error bars indicating one standard deviation.

slightly more positive isomer shifts indicating an increase in electron density at the iron nuclei. The data collected at 25 K can be modelled as a 41(2) : 59(2) mixture of a singlet and a sextet, the latter indicating the presence of an internal magnetic field which is static on the Mössbauer timescale of 10–100 ns. On cooling the sample to 10 K the fraction of iron nuclei which are experiencing a static field has increased to 88(2)%. The

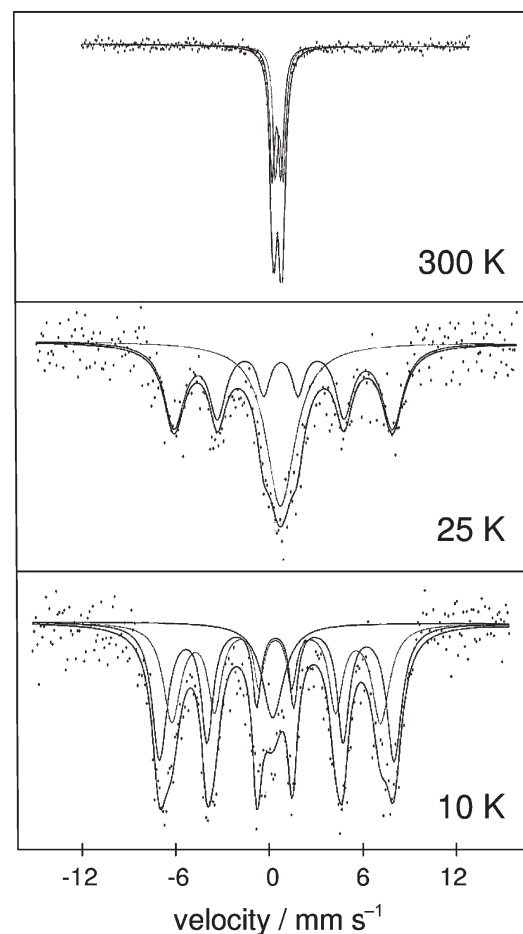


Fig. 4 The observed (dots) and simulated (line) Mössbauer spectra collected from $\text{Sr}_4\text{FeMoO}_8$ at 300 K, 25 K and 10 K.

results from the fitted Mössbauer spectroscopy data are collected in Table 3.

Having identified the presence of a small quantity of metallic iron in sample **A** indicating the sample had been slightly over-reduced, sample **B** was prepared. X-Ray diffraction collected from **B** showed that this sample was a single phase $n = 1$ Ruddlesden–Popper phase and the data could be fitted, as shown in Fig. 5, using a single phase model. Magnetic susceptibility data collected from **B** showed no evidence of the ferromagnetic impurity which had dominated the bulk magnetic properties of **A**. The data from **B** could be fitted satisfactorily to the Curie–Weiss law in the range $80 \leq T/\text{K} \leq 300$ as shown in Fig. 6, yielding values for C and θ of $2.134(4) \text{ cm}^3 \text{ K mol}^{-1}$ and $1.2(2) \text{ K}$ respectively. The Curie constant is associated with a paramagnetic moment of $4.13(1) \mu_{\text{B}}$. The magnetisation of $\text{Sr}_4\text{FeMoO}_8$ shows no history dependence for temperatures above $16(1) \text{ K}$. At this temperature the zero-field cooled data pass through a maximum whilst the field-cooled magnetisation continues to increase on cooling further.

Discussion

The formation of impurities in sample **A** but not in sample **B** suggests that a degree of molybdenum loss occurs during the

Table 3 The electronic parameters used to model the Mössbauer spectroscopy data collected from $\text{Sr}_4\text{FeMoO}_8$

T/K	No. of lines	Isomer shift $\delta/\text{mm s}^{-1}$	Quadrupole splitting $\Delta/\text{mm s}^{-1}$	Relative area
300	2	0.31(1)	−0.58	0.51
	2	0.49(1)	−0.51	0.49
77	2	0.42(2)	−0.58	0.44
	2	0.61(1)	−0.55	0.56
25	1	0.55(3)	—	0.41
	6	0.61(2)	0.16	0.59
10	1	0.38(8)	—	0.12
	6	0.56(3)	0.07	0.40
	6	0.59(2)	0.12	0.48

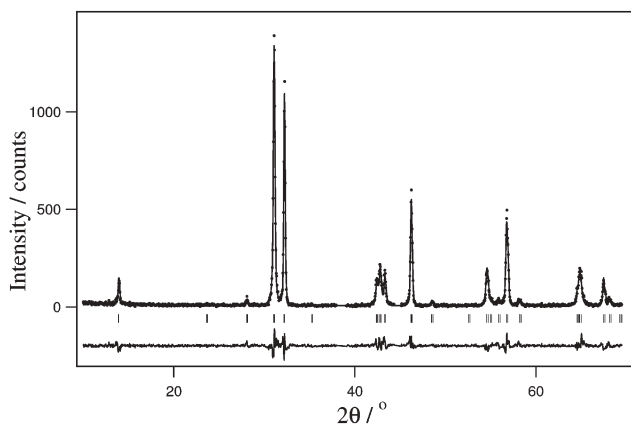


Fig. 5 Observed (dots), calculated (line) and difference X-ray powder diffraction patterns collected from sample **B** at room temperature. The tick marks indicate allowed Bragg peaks. Excluded regions contain Bragg peaks from the aluminium sample holder.

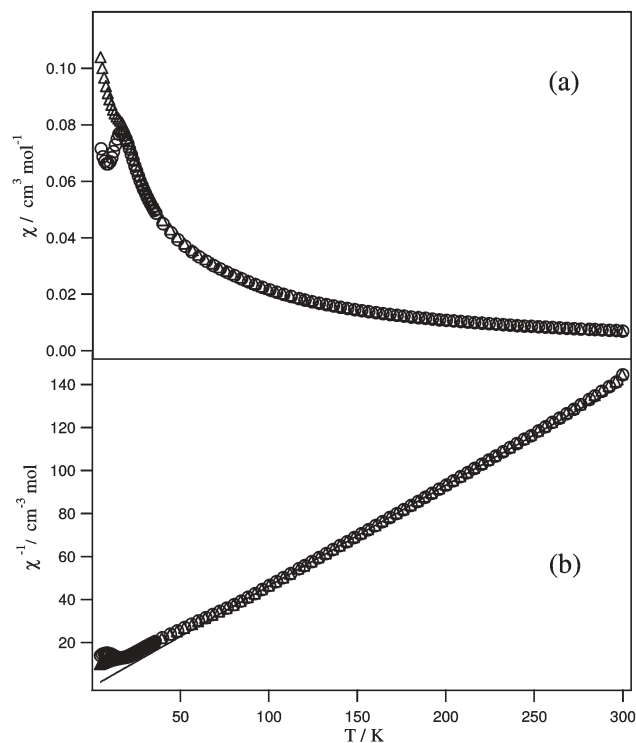


Fig. 6 (a) Magnetic susceptibility of $\text{Sr}_4\text{FeMoO}_8$ collected after cooling the sample in zero field (circles) and in the measuring field of 1000 G (triangles). (b) The inverse magnetic susceptibility fitted to the Curie–Weiss law in the temperature range $80 \leq T/\text{K} \leq 300$.

synthesis of $\text{Sr}_4\text{FeMoO}_8$. Similar high temperature preparative routes have been widely employed^{2,5,22,23} in the synthesis of the parent perovskite phases A_2MMoO_6 without any report of Mo loss. This loss presumably occurs during the initial stage of the heat treatment due to the volatility of MoO_3 (melting point = $795 \text{ }^\circ\text{C}$). Refinement of the Fe/Mo fractional occupancy against the X-ray powder diffraction data showed the sample was stoichiometric in iron and molybdenum. However, the quality of the fit was not significantly degraded by small adjustments to the stoichiometry suggesting that the stoichiometry could vary within the range $\text{Sr}_4\text{Fe}_{1.0(1)}\text{Mo}_{0.9(1)}\text{O}_8$ whilst having negligible impact on the resulting X-ray diffraction pattern. As both the X-ray diffraction data and magnetometry measurements failed to find any evidence of a second phase, the stoichiometry of sample **B** can be assumed to be close to the ideal $\text{Sr}_4\text{FeMoO}_8$.

Both X-ray and neutron powder diffraction data show that this compound adopts the ideal single layer Ruddlesden–Popper phase and thus contains Fe and Mo in a disordered manner on a single octahedrally-coordinated site. The mean ionic radii²⁴ of the possible ion pairs $\text{Fe}^{2+}/\text{Mo}^{6+}$ and $\text{Fe}^{3+}/\text{Mo}^{5+}$ have values of 0.685 and 0.628 \AA respectively and so information on the oxidation states of the transition metals can be extracted by an examination of the transition-metal–oxide distances. The mean metal–oxide bond length of $1.9814(7) \text{ \AA}$ is intermediate between the mean distances of 1.987 \AA and 1.973 \AA reported⁵ for Fe–O and Mo–O respectively in the tetragonal, cation-ordered phase $\text{Sr}_2\text{FeMoO}_6$ at 200 K and is close to the mean of these two values (1.980 \AA). Reference to

neutron powder diffraction studies^{12,25} of $\text{Sr}_2\text{Fe}^{\text{II}}\text{W}^{\text{VI}}\text{O}_6$ and $\text{Sr}_2\text{Mn}^{\text{II}}\text{Mo}^{\text{VI}}\text{O}_6$ carried out at room temperature yields typical bond lengths of $\text{Fe}^{2+}\text{-O}$ (2.083 Å) and $\text{Mo}^{6+}\text{-O}$ (1.920 Å) respectively. The mean metal–oxide bond length which would be anticipated for a $\text{Fe}^{2+}/\text{Mo}^{6+}$ ion pair would be *ca.* 2.002 Å and our data thus suggest that the octahedrally coordinated sites are occupied by $\text{Fe}^{3+}/\text{Mo}^{5+}$ rather than the alternative $\text{Fe}^{2+}/\text{Mo}^{6+}$ couple. Whilst cation ordering over octahedral sites has been observed^{15,17,26} for Ruddlesden–Popper phases, it is well established that cation pairs which order in the perovskite parent materials do not always order in the layered analogues. In some cases,¹⁵ cation ordering can occur within the perovskite layers but the ordering between the layers is randomised leading to a quasicrystalline phase. The diffraction data do not preclude such a situation and so the local environments around the iron nuclei were examined using Mössbauer spectroscopy.

Mössbauer spectroscopy is invaluable in probing the local ordering patterns around the FeO_6 octahedra. Two limiting cases of cation ordering can be considered; (i) the system shows complete order between FeO_6 and MoO_6 within the layers and (ii) the cations within the layers have a wholly random arrangement of FeO_6 and MoO_6 octahedra as neighbours. In (i) each iron nucleus will experience the same environment and so a single resonance would be observed in the Mössbauer spectrum. If (ii) occurs then any iron nucleus could have between zero and four neighbouring MoO_6 octahedra and for the case of two neighbours these could be in *cis* or *trans* geometries resulting in a total of six possible iron nuclear environments. Due to the limited resolution of the Mössbauer technique and the subtle differences between these different environments it is not possible to distinguish between these six sites experimentally. Nevertheless, the requirement of two Fe resonances in fitting the Mössbauer spectroscopy data collected at room temperature clearly indicates that this material does not exhibit cation order but can be described as a fully cation-disordered system. This absence of cation order in $\text{Sr}_4\text{FeMoO}_8$ can be ascribed to the reduction in nearest-neighbouring transition metal octahedra from six, in the (cation-ordered) perovskite, to four, in the $n = 1$ Ruddlesden–Popper structure. The reduction in the number of neighbouring octahedra reduces the electrostatic energy and mechanical strain associated with a disordered cation arrangement and allows the entropy gain associated with a random placement of FeO_6 and MoO_6 octahedra to determine the adopted structure.

The Mössbauer spectroscopy also permits an estimation of the oxidation state of the iron in $\text{Sr}_4\text{FeMoO}_8$. At room temperature the resonances lie in the range of isomer shifts typical for Fe^{3+} in octahedral coordination,^{27,28} providing confirmation of the $\text{Fe}^{3+}/\text{Mo}^{5+}$ valence suggested by the metal–oxide bond lengths derived from the neutron diffraction data. On cooling the sample, the isomer shifts increase and approach the upper boundary of the range of values expected for high spin Fe^{3+} . A similar increase in isomer shift has been observed²⁹ on cooling $\text{Sr}_2\text{FeMoO}_6$ and was ascribed to partial electron transfer from Mo^{5+} to Fe^{3+} resulting in the formation of the non-integer oxidation state of $\text{Fe}^{2.5+}$. On cooling $\text{Sr}_4\text{FeMoO}_8$ further, the isomer shift continues to increase

but never reaches the values associated with the formation of high-spin divalent iron. The presence of a static, internal magnetic field in the sample at 25 K and to a greater extent at 10 K indicates that the material is no longer in the paramagnetic regime at these temperatures and would suggest the formation of a magnetically ordered phase. Such a magnetic transition is compatible with the maximum in the magnetic susceptibility observed at 16(1) K. The divergence observed below this temperature is a clear indication that the magnetic moments of the transition metals are no longer dynamic but that magnetic interactions within the sample dominate over the thermal energy below this temperature. The difference in magnetic transition temperature determined by the two techniques stems from the different timescales of the two experiments. Mössbauer spectroscopy samples the environment of the iron nucleus over a timescale²¹ of 10–100 ns whilst the susceptibility measurements record the bulk magnetisation over several minutes. The observation at 25 K of 59(1)% of Fe nuclei experiencing a magnetic field which is static on the Mössbauer timescale is thus compatible with the observation of bulk paramagnetism persisting down to 16 K on the timescale of a magnetisation measurement. The susceptibility data above the transition can be fitted using the Curie–Weiss law to yield a value for the paramagnetic moment, $4.13 \mu_{\text{B}}$, substantially lower than that expected for either $\text{Fe}^{3+}/\text{Mo}^{5+}$ (spin-only $\mu = 6.16 \mu_{\text{B}}$) or $\text{Fe}^{2+}/\text{Mo}^{6+}$ ($\mu_{\text{so}} = 4.89 \mu_{\text{B}}$) ion pairs. The Weiss constant resulting from this fit, $\theta = 1.2$ K, could be interpreted as signifying that the interactions between magnetic centres are extremely weak and ferromagnetic. However, such an assignment is incompatible with the observation of a magnetic transition at 16 K. The Weiss constant should represent the averaged magnetic interactions between the paramagnetic centres and, in an ideal model, the magnetic centres should undergo magnetic ordering at a temperature of similar magnitude to the Weiss constant. The observation of a magnetic transition at a temperature so much higher than the Weiss constant indicates the match between the susceptibility of $\text{Sr}_4\text{FeMoO}_8$ and the Curie–Weiss law is serendipitous and that the derived magnetic parameters are without physical basis. Similar observations have been made in spin-glass systems³⁰ which have illustrated the potential pitfalls of assigning too great a significance to the results of Curie–Weiss fits to magnetic susceptibility data obtained from magnetically concentrated, disordered systems.

Neutron diffraction data from $\text{Sr}_4\text{FeMoO}_8$ collected below 16 K show that the magnetic transition observed in the susceptibility measurements is due to the formation of a spin-glass phase and that this material exhibits no long-range magnetic order at 1.7 K. The only evidence of a magnetic transition in the neutron diffraction data is a reduction in a M–O bond distance on heating the sample to 17 K. Similar adjustments³¹ in bond length are often reported around magnetic ordering temperatures and the magnetostrictive effect observed in the present case is presumably related to a reduction in electron repulsion associated with short range spin correlations in the spin-glass phase. No significant change in the anisotropic displacement parameters of the oxide ions was observed as a function of temperature around the magnetic transition. The formation of a spin-glass phase at

16(1) K in $\text{Sr}_4\text{FeMoO}_8$ is in stark contrast to the parent perovskite $\text{Sr}_2\text{FeMoO}_6$ which forms a long-range ferrimagnetically ordered phase below a magnetic transition temperature of ca. 420 K. It has been shown in $\text{Sr}_3\text{Fe}_2\text{O}_{7-\delta}$ that two-dimensional magnetic order can exist in RP phases at 110 K²⁷ and so the change from a three-dimensional perovskite to a two-dimensional RP structure is not responsible for the change in magnetic properties in the Fe/Mo compounds. Instead, this dramatic difference in physical properties stems from the difference in chemical ordering between the two phases. The presence of cation disorder in $\text{Sr}_4\text{FeMoO}_8$ leads to a randomisation in the exchange interactions between neighbouring cations and thus disrupts the formation of a magnetically ordered phase. Below 16 K the magnetic moments on individual cation sites adopt orientations such that the exchange energy with their neighbours is minimised. However, the cation disorder identified by the diffraction experiments and Mössbauer spectroscopy measurements means that these orientations are not propagated through the structure but instead are a function of the random placement of Fe^{3+} and Mo^{5+} throughout the sample. The net exchange interaction experienced by each magnetic centre will therefore be greatly reduced leading to the observed reduction in the magnetic transition temperature.

Conclusions

X-Ray and neutron powder diffraction combined with Mössbauer spectroscopy have shown that Fe^{3+} and Mo^{5+} are disordered over the octahedral sites of $\text{Sr}_4\text{FeMoO}_8$ over all length scales. This has a dramatic impact on the magnetic properties of this phase compared to the parent perovskite. Whereas $\text{Sr}_2\text{FeMoO}_6$ exhibits ferrimagnetic order below 420 K, $\text{Sr}_4\text{FeMoO}_8$ forms a magnetically disordered phase below the transition temperature of 16(1) K. The origin of this reduction in the net magnetic exchange is the chemical disorder between the transition metals leading to a randomisation of the magnetic interactions. Hence individual cations are subjected to conflicting exchange interactions and remain dynamically disordered at temperatures down to 16 K and statically disordered below this temperature. The key to achieving ferrimagnetism and magnetoresistance in the RP phases will be to increase the stabilisation of a cation-ordered arrangement with respect to the disordered structure observed in $\text{Sr}_4\text{FeMoO}_8$. Work is ongoing to prepare the higher-order RP phases with thicker perovskite blocks and hence an increased number of neighbouring octahedra in an effort to induce order between the FeO_6 and MoO_6 octahedra and the desired electronic properties.

Acknowledgements

We are grateful to the Royal Society for provision of a University Research Fellowship and a grant to support this research and to Dr R. I. Smith at ISIS, Rutherford Appleton Laboratories for experimental assistance with the neutron powder diffraction experiments.

Edmund J. Cussen^{a*} and Mike F. Thomas^b

^aThe School of Chemistry, The University of Nottingham, University Park, Nottingham, UK NG7 2RD.

E-mail: edmund.cussen@nottingham.ac.uk; Tel: +44 115 951 3503

^bThe Department of Physics, The University of Liverpool, Liverpool, UK L69 7ZE

References

- 1 F. Galasso, F. C. Douglas and R. Kasper, *J. Chem. Phys.*, 1966, **44**, 1672.
- 2 K.-I. Kobayashi, T. Kimura, H. Sawada, K. Terakura and Y. Tokura, *Nature*, 1998, **395**, 677.
- 3 H. Yanagihara, M. B. Salamon, T. Lyanda-Geller, S. Xu and Y. Moritomo, *Phys. Rev. B*, 2001, **64**, 214407.
- 4 D. D. Sarma, *Curr. Opin. Solid State Mater. Sci.*, 2001, **5**, 261.
- 5 C. Ritter, M. R. Ibarra, L. Morellon, J. Blasco, J. Garcia and J. M. De Teresa, *J. Phys.: Condens. Matter*, 2000, **12**, 8295.
- 6 M. J. Martinez-Lope, J. A. Alonso, M. T. Casais and M. T. Fernandez-Diaz, *Eur. J. Inorg. Chem.*, 2002, 2463.
- 7 M. J. Martinez-Lope, J. A. Alonso and M. T. Casais, *Z. Naturforsch., B: Chem. Sci.*, 2003, **58**, 571.
- 8 T. S. Chan, R. S. Liu, G. Y. Guo, S. F. Hu, J. G. Lin, J. M. Chen and J. P. Attfield, *Chem. Mater.*, 2003, **15**, 425.
- 9 K. I. Kobayashi, T. Kimura, Y. Tomioka, H. Sawada, K. Terakura and Y. Tokura, *Phys. Rev. B*, 1999, **59**, 11159.
- 10 S. Nomura and T. Nakagawa, *J. Phys. Soc. Jpn.*, 1966, **21**, 1068.
- 11 M. C. Viola, M. J. Martinez-Lope, J. A. Alonso, P. Velasco, J. L. Martinez, J. C. Pedregosa, R. E. Carbonio and M. T. Fernandez-Diaz, *Chem. Mater.*, 2002, **14**, 812.
- 12 A. K. Azad, S.-G. Eriksson, S. A. Ivvanov, R. Mathieu, S. P. Svedlindh, J. Eriksen and H. Rundlof, *J. Alloys Compd.*, 2004, **364**, 77.
- 13 G. Blasse, *Philips Res. Rep.*, 1965, **20**, 327.
- 14 G. M. Veith, M. V. Lobanov, T. J. Emge, M. Greenblatt, M. Croft, F. Stowasser, J. Hadermann and G. van Tendeloo, *J. Mater. Chem.*, 2004, **14**, 1623.
- 15 J. C. Burley, P. D. Battle, D. J. Gallon, J. Sloan, C. P. Grey and M. J. Rosseinsky, *J. Am. Chem. Soc.*, 2002, **124**, 620.
- 16 G. Demazeau, E. O. Ohkim, K. T. Wang, L. Fournes, J. M. Dance, M. Pouchard and P. Hagenmuller, *Rev. Chim. Mineral.*, 1987, **24**, 183.
- 17 S. A. Warda, W. Massa, D. Reinen, Z. Hu, G. Kaindl and F. M. F. d. Groot, *J. Solid State Chem.*, 1999, **146**, 79.
- 18 Y. Moritomo, A. Asamitsu, H. Kuwahara and Y. Tokura, *Nature*, 1996, **380**, 141.
- 19 H. M. Rietveld, *Acta Crystallogr.*, 1969, **2**, 65.
- 20 A. C. Larson and R. B. von Dreele, *General Structure Analysis System (GSAS)*, Los Alamos National Laboratories, Los Alamos, NM, 1990.
- 21 N. N. Greenwood and T. C. Gibb, *Mössbauer Spectroscopy*; Chapman and Hall Ltd., London, 1971.
- 22 Y. Moritomo, S. Xu, A. Machida, T. Akimoto, E. Nishibori, M. Takata and M. Sakata, *Phys. Rev. B*, 2000, **61**, R7827.
- 23 M. S. Moreno, J. E. Gayone, M. Abbate, A. Caeiro, D. Niebieskikwiat, R. D. Sanchez, A. de Siervo, R. Landers and G. Zampieri, *Solid State Commun.*, 2001, **120**, 161.
- 24 R. D. Shannon, *Acta Crystallogr. Sect. A: Cryst. Phys., Diffr., Theor. Gen. Cryst.*, 1976, **32**, 751.
- 25 A. K. Azad, S.-G. Eriksson, A. Mellergard, A. A. Ivanov, J. Eriksen and H. Rundlof, *Mater. Res. Bull.*, 2002, **37**, 1797.
- 26 P. D. Battle, J. C. Burley, D. J. Gallon, C. P. Grey and J. Sloan, *J. Solid State Chem.*, 2004, **177**, 119.
- 27 S. E. Dann, M. T. Weller, D. B. Currie, M. F. Thomas and A. D. Alrawwas, *J. Mater. Chem.*, 1993, **3**, 1231.
- 28 P. D. Battle, C. M. Davison, T. C. Gibb and J. F. Vente, *J. Mater. Chem.*, 1996, **6**, 1187.
- 29 J. Linden, T. Yamamoto, M. Karppinen, H. Yamuchi and T. Pieterari, *Appl. Phys. Lett.*, 2000, **76**, 2925.
- 30 E. J. Cussen and P. D. Battle, *J. Mater. Chem.*, 2003, **13**, 1210.
- 31 C. S. Knee, D. J. Price, M. R. Lees and M. T. Weller, *Phys. Rev. B: Condens. Matter*, 2003, **B68**, 174407.